Heliyon 10 (2024) e32773

Contents lists available at ScienceDirect

Heliyon

journal homepage: www.cell.com/heliyon

Research article

# Genome-scale identification, expression and evolution analysis of *B-box* members in *Dendrobium huoshanense*

Hui Deng [a], Yingyu Zhang [b], Muhammad Aamir Manzoor [c], Irfan Ali Sabir [d], Bangxing Han [a,**], Cheng Song [a,*]

[a] *Anhui Dabieshan Academy of Traditional Chinese Medicine, Anhui Engineering Research Center for Eco-Agriculture of Traditional Chinese Medicine, College of Biological and Pharmaceutical Engineering, West Anhui University, Luan, 237012, China*
[b] *Henan Key Laboratory of Rare Diseases, Endocrinology and Metabolism Center, The First Affiliated Hospital, and College of Clinical Medicine of Henan University of Science and Technology, Luoyang, 471003, China*
[c] *Department of Plant Science, School of Agriculture and Biology, Shanghai Jiao Tong University, Shanghai, 201109, China*
[d] *Guangdong Provincial Key Laboratory of Postharvest Science of Fruits and Vegetables/Key Laboratory of Biology and Genetic Improvement of Horticultural Crops, Ministry of Agriculture and Rural Affairs, College of Horticulture, South China Agricultural University, Guangzhou, 510642, China*

A B S T R A C T

B-box (BBX) proteins have been recognized as vital determinants in plant development, morphogenesis, and adaptive responses to a myriad of environmental stresses. These zinc-finger proteins play a pivotal role in various biological processes. Their influence spans photomorphogenesis, the regulation of flowering, and imparting resilience to a wide array of challenges, encompassing both biotic and abiotic factors. Chromosome localization, gene structure and conserved motifs, phylogenetic analysis, collinearity analysis, expression profiling, fluorescence quantitative analysis, and tobacco transient transformation methods were used for functional localization and expression pattern analysis of the *DhBBX* gene. A total of 23 *DhBBX* members were identified from *Dendrobium huoshanense*. Subsequent phylogenetic evaluations effectively segregated these genes into five discrete evolutionary subsets. The predictions of subcellular localizations revealed that all these proteins were localized in the nucleus. The genetic composition and patterns showed that the majority of these genes consisted of several exons, with a few variations that could be attributed to transposon insertion. A comprehensive analysis using *q*RT-PCR was conducted to unravel the expression patterns of these genes in *D. huoshanense*, with a specific concentration on their responses to various hormone treatments and cold stress. Subcellular localization reveals that *DhBBX21* and *DhBBX9* are located in the nucleus. Our results provide a deep comprehension of the complex regulatory mechanisms of BBXs in response to various environmental and hormonal stimuli. These discoveries encourage further detailed and focused investigations into the operational dynamics of the *BBX* gene family in a wider range of plant species.

## 1. Introduction

Transcription factors (TFs) are pivotal in orchestrating a spectrum of plant biological processes, encompassing developmental regulation, stress adaptation, and the modulation of secondary metabolic pathway [1]. It is possible to categorize TFs into different groups based on their ability to bind *cis*-acting elements to the promoter regions. One of the most significant groups of transcription factors (TFs) in plants is the zinc finger family. In accordance with the structural and functional characteristics of each of its individual members, zinc finger TFs are divided into a number of subfamilies [2]. Within this group, B-box proteins (BBXs) constitute a subset of

* Corresponding author.
** Corresponding author.
*E-mail addresses:* hanbx1978@sina.com (B. Han), lanniao812329218@163.com (C. Song).

https://doi.org/10.1016/j.heliyon.2024.e32773
Received 10 December 2023; Received in revised form 24 May 2024; Accepted 9 June 2024
Available online 10 June 2024

zinc-finger transcription factors. Regardless of whether they feature a C-terminal CCT (CO-like, TOC1, and CONSTANS) domain, BBX proteins consistently contain one or more N-terminal B-box domains, which play pivotal roles in transcriptional regulation, protein interactions, and nuclear transport [3,4]. In *A. thaliana*, the BBX family has undergone a comprehensive identification and classification process, resulting in the categorization of its 32 members into four groups. This classification is based on the number of B-box domains and the presence or absence of a CCT domain [5].

Members of Groups I and II within the *AtBBX* family are characterized by the presence of two B-box domains, accompanied by a CCT domain. Conversely, Group III members are characterized by a combination of a single B-box domain and a CCT domain. In Group IV, there are two B-box domains, but they lack a CCT domain. Group V, on the other hand, is defined by a single B-box domain [6]. Numerous plants, including Arabidopsis [5], rice [7], pear [8], pepper [9], tomato [10], and wolfberry [11], have identified BBX genes. Segmental duplication and deletion events over evolutionary time have resulted in variations in the consensus sequences of the two B-box domains [12]. The remarkably conserved CCT domain, which spans a range of 42–43 amino acids, plays a critical role in the control of transcriptional functions and the transport of nuclear proteins [13]. Recent genome-wide expression analyses suggest that BBX proteins may play a role in plant hormone signaling responses. Specifically, abscisic acid (ABA), a hormone released by plants in response to stress, has been implicated in modulating the expression of BBX genes [14]. Microarray studies have shown differential expression of *BBX* genes in response to ABA [15,16]. Furthermore, extensive research has demonstrated the critical involvement of *BBX* genes in regulating various aspects of plant biology, including growth, development, flowering, and the plant's response to abiotic stress [17,18].

Currently, the scientific community is increasingly intrigued by B-box proteins, recognizing their evolving role in various plant growth processes. Previous studies have cataloged the expression patterns of the BBX family in *Oryza sativa*, especially in relation to certain hormonal responses [19]. However, there are few studies on the BBX family under abiotic stresses in Dendrobium plants. *D. huoshanense*, a semi-shaded perennial plant from the *Orchidaceae* family, is commonly found in various environments, both natural and cultivated, often encounters challenging conditions such as elevated high temperatures, cold stress, drought stress, and additional stressors [20–22]. *D. huoshanense* is also a valuable Chinese herbal medicine. The polysaccharides in it have significant anti-tumor and immunity-improving effects [23]. Exposure to stress can reduce a plant's ability to tolerate adverse conditions, potentially leading to a significant decrease in productivity. Throughout their life cycle, plants face numerous challenges arising from environmental factors such as low temperatures, drought, salinity, and biotic stressors. These stressors can negatively impact plant growth and development, ultimately affecting overall productivity [24,25]. Such stressful situations result in unfavorable environmental circumstances for growth, development, and productivity. In response to environmental stimuli, plants rely on transcriptional regulation of gene expression for numerous physiological and metabolic functions. This includes reactions to multiple stressors such as salinity, cold, and drought, as well as defensive mechanisms against microbial invasions [26]. These TFs may have the ability to regulate gene expression at the molecular level by maintaining, promoting, and suppressing it. Furthermore, there is limited knowledge regarding the functions of the BBX family in the evolutionary relationship, structural modifications, stress responses, and functional variability of these proteins in *D. huoshanense*. As a result, the 23 members of the BBX family in *D. huoshanense* and their patterns of expression under five hormone treatments and cold stress were comprehensively examined in the current work. These results provide valuable insights into the evolutionary history of *BBXs* in *D. huoshanense*, shedding light on their potential biological functions related to multiple abiotic stress responses and plant growth regulation.

## 2. Materials and methods

### 2.1. Plant sampling and tissue preservation

*D. huoshanense* seedlings were obtained from the Plant Cell Engineering Center at West Anhui University (Luan, China). All samples utilized for the treatment of plant hormone assays were maintained at room temperature with 60 % relative humidity and subjected to long-day conditions, comprising 12 h of light followed by 12 h of darkness. Plants with uniform growth rates and ages were chosen for the study. Leaves were sprayed with water and 50 mmol/L MeJA solution, respectively. Time intervals between sprays were set at 0.25 h, 0.5 h, 1 h, 2 h, 4 h, 8 h, and 16 h. Leaves from both the control and MeJA-treated groups were harvested at distinct time points, immediately frozen in liquid nitrogen, and subsequently stored in a −80 °C freezer for future analysis.

### 2.2. Identification and characterization of BBX encoding genes in the genome of D. huoshanense

Two distinct approaches were utilized to find the genes that encode BBXs in the *D. huoshanense* genome. The first method used was retrieving the established sequences of AtBBXs from the TAIR database. Afterwards, we utilized these sequences to conduct a search for putative BBXs in the *D. huoshanense* genome database using the BLASTP tool, with the E value limit set at $1e^{-3}$. The second method involved acquiring the hidden Markov model (HMM) profile of the BBX domain (Pfam00643) from the Pfam database. Subsequently, the HMM profile was employed to find all BBXs in the *D. huoshanense* genome using HMMER 3.0 software, with an E value cutoff of $1e^{-3}$ [27–30]. The Arabidopsis BBX gene family was obtained from the TAIR 10 database (https://www.arabidopsis.org/browse/genefamily/index.jsp). To assess the completeness of protein sequences and the existence of specific domains, we employed the following online resources: SMART (http://smart.embl-heidelberg.de/) (Schultz et al., 1998), InterPro Scan (http://www.ebi.ac.uk/interpro/), the Conserved Domain Database (CDD) (http://www.ncbi.nlm.nih.gov/cdd/), and ScanProsite (http://prosite.expasy.org/scanprosite/). Through the ExPASy online server (http://web.expasy.org/protparam/), the chemical characteristics of BBX proteins were investigated, including the instability index, protein length, aliphatic index, isoelectric point, molecular weight, and grand

average of hydrophobicity [31,32]. The precise position of the *DhBBXs* gene on the associated chromosomes was depicted using TBtools and MapDraw software. The physical and chemical characteristics of the *D. huoshanense* B-box protein sequence, including isoelectric point and molecular weight predictions, were examined using the Expasy website (http://expasy.org) [3]. By entering the amino acid sequence of the DhBBX family, the subcellular position was determined using the web program Cell-PLoc 2.0 (http://www.csbio.sjtu.edu.cn/bioinf/Cell-PLoc-2/).

### 2.3. Gene structure and motif analysis of DhBBX genes

A multi-gene family's evolution may be facilitated by gene structural variety, according to earlier studies. Gene exon-intron analysis was done to further characterize and comprehend the structural variety of *DhBBX* genes. The *DhBBX* genes were investigated and characterized using a systematic approach. The motifs present in each DhBBX gene were meticulously analyzed through the MEME suite (http://meme-suite.org/tools/meme). To visualize the outcomes, the Gene Structure View tool included in the TBtools package was utilized. The motif identifications were set as follows: each motif was expected to have a width ranging from 6 to 200, with a maximum limit of 20 motifs. Furthermore, the gene structures pertaining to *DhBBX*s were delineated using the essential nucleotide sequence, and this analysis was performed by the online website GSDS software (http://gsds.gao-lab.org/).

### 2.4. Phylogenetic analysis of DhBBX and AtBBX proteins

Using ClustalW software, the sequence alignment of BBX proteins from *D. huoshanense* and *A. thaliana* was employed [33]. The Maximum Likelihood Method (MLM) was used to create the phylogenetic tree using the MEGA X program [34]. One thousand replicates used in the bootstrap analysis by usinig iTOL v6.0 (https://itol.embl.de/itol_account.cgi) were utilized to show the phylogenetic trees [35].

### 2.5. Gene duplication and collinearity analysis of DhBBX genes

The MCScanX software was utilized to identify *BBX* gene duplications both intraspecifically and interspecifically. Gene duplication events were determined based on the following parameters: (1) The aligned segment of the two gene sequences extends beyond 80 % of the length of the longer sequence; (2) Among genes in close relation, each participated in WGD or segmental duplication event [36]. By doing an enrichment analysis and applying Fisher's exact test, it was possible to determine the relationship between the number of gene families and a specific genome-wide duplication mechanism [37]. Using a pipeline that has been described, the Ka and Ks values of duplicated gene pairs were determined. The analysis of gene duplication and synteny was executed using the MCscanX software and TBtools software. The exploration of synteny relationships of *DhBBX* genes among *D. huoshanense*, *O. sativa, A. thaliana, D. nobile,* and *D. chrysotoxum* was undertaken and subsequently visualized employing the MCScanX toolkit.

### 2.6. Cis-acting element analysis of DhBBX genes

To find out the potential *cis*-acting elements in the promoter regions of the *DhBBX* genes, 2000bp DNA sequences from the predicted start of transcription were downloaded from the *D. huoshanense* genome. These sequences were subsequently analyzed using the PlantCARE database (http://bioinformatics.psb.ugent.be/webtools/plantcare/html/) for the identification of multiple elements in the *DhBBX* gene promoter [38]. Finally, TBtools software was used for visualization [39].

### 2.7. Expression profile and transcriptomic analysis of DhBBX genes

To evaluate the expression levels of *DhBBX* genes, we extracted the fragments per kilobase of exon model per million mapped fragments (FPKM) values from pre-existing transcriptome datasets accessible on the Genome Sequence Archive (GSA) under the accession number CRA006607 (https://ngdc.cncb.ac.cn/gsa/browse/). The computation of these values employed the Salmon tool in conjunction with RNA-seq data [40]. By standardizing the $\log_2$ (FPKM) values for all unigenes, a structured framework was established for hierarchical clustering and the delineation of *DhBBX* gene expression patterns. To conduct an extensive correlation analysis of *DhBBX* genes, we employed the SupCorrPlot tool integrated into the TBtools software suite. This allowed us to calculate Spearman correlation coefficients and their corresponding significance values.

### 2.8. Expression patterns of DhBBXs under various stress conditions via qRT-PCR method

RNA extraction was conducted using the QIAGEN RNA extraction kit from Germany. To ensure the purity of the RNA samples, any remaining genomic DNA was removed using the RNAse-Free DNase Set (QIAGEN, Germany). Subsequently, the quality and integrity of these RNA samples were assessed through the NanoDrop 2000c spectrophotometer (Thermo Fisher Scientific, USA) and gel electrophoresis. For the conversion of RNA into complementary DNA, the synthesis of cDNA was employed, and the reverse transcription reaction is performed by using PrimeScriptTM II 1st Strand cDNA Synthesis Kit (TaKaRa, Dalian, China). Quantitative real-time PCR (*q*RT-PCR) was performed on the 7500 Series Real-Time Fluorescence Quantitative Cycler (Bio-RAD, USA), utilizing the SYBR Premix Ex TaqTM II from TaKaRa (Dalian, China). The Actin gene was selected as the internal control to normalize the results. The *q*RT-PCR primers were designed using Primer Premier 5.0 software, with detailed information available in Table S1. The expression patterns of

the BBX genes under investigation were determined employing the comparative threshold cycle method ($2^{-\Delta\Delta Ct}$) as described by Ref. [41]. To ensure robustness, each experimental step was meticulously conducted in triplicate.

### 2.9. Subcellular localization of DhBBX21 and DhBBX9

The homologous recombination primers of the pCAMBIA1305 vector were designed using the homologous recombination method. The homologous primers with XbaI and BamHI sites were presented. The designed homologous primers were used to clone the target fragment. The pCAMBIA1305 empty plasmid was double-digested according to the restriction sites of XbaI and BamHI. The digested carrier fragments were determined by gel electrophoresis. After the homologous recombination reaction between the target fragment and the vector fragment, the recombinant eukaryotic expression plasmid was constructed and successfully obtained. The recombinant vector plasmid was extracted for PCR detection and sequencing. The pCAMBIA1305 plasmid recombined with the target fragment was introduced into *Agrobacterium* GV3101, and positive single clones were picked out by streaking, and used to infect tobacco after expanding culture. The infection solution used was 10 mmol/L $MgCl_2$, 200 μmol/L AS (acetosyringone), and 10 nmol/L morpholineethanesulfonic acid (MES) (pH 5.5). The bacterial liquid was centrifuged at 6000 rpm/min for 10 min to collect the bacteria. After mixing the infection solution with the bacteria, the OD600 value was 0.6–0.8, and the cells were cultured in the dark for 3 h. Tobacco leaves were selected for injection on the back side and cultured in the dark for 3 days. The infected parts of the leaves were removed to make slices and observed under a confocal laser microscope.

## 3. Results

### 3.1. Identification, physiochemical properties, and chromosomal localization analysis of BBX genes

To identify the *BBX* genes from the *D. huoshanense* genome, the HMMER and Pfam softwares were used for the HMM profiles of both the BBox and CCT domains (Finn et al., 2014). The conserved CCT and BBox domains were then verified using SMART, InterPro, and Pfam databases. Finally, 23 BBox genes were identified after removing the split and duplicated *DhBBXs* (Table 1). Additionally, the online program Expasy Protoparam (http://www.expasy.org/tools/protparam.html) was used to research the physiochemical properties such as the length of the amino acid sequence of BBX members (Table 1). The BBX gene family presumed molecular weights range greatly, from 15992.6 Da (Dhu000014192) to 55543.31 Da (Dhu000010883). The calculated overall hydropathicity, isoelectric point, alphabetic index, and instability index, values ranged from 4.6 to 8.42, 44.43 to 73.99, 51.81 to 96.37, and −0.746 to 0.19, respectively. Subcellular localization prediction shows that all DhBBX proteins are localized in the nucleus.

### 3.2. Phylogeny analysis of DhBBXs and ATBBXs

An evolutionary tree was constructed to depict the relationship between BBX proteins of *D. huoshanense* and *A. thaliana*, employing the Maximum Likelihood (ML) method. Based on bootstrap value and sequence homology of the phylogenetic tree, combined with Arabidopsis nomenclature, the categorization of BBX genes into five distinct families: I, II, III, IV and V. BBX proteins can be

**Table 1**
Physiochemical properties sequence characteristics of 23 *B-Box* identified in *D. huoshanense*.

| Sequence ID | Gene Renaming | Number of Amino Acid | Molecular Weight | Theoretical pI | Instability Index | Aliphatic Index | Grand Average of Hydropathicity | Subcellular localization |
|---|---|---|---|---|---|---|---|---|
| Dhu000000904 | DhBBX3 | 332 | 35540.86 | 5.7 | 46.56 | 63.64 | −0.234 | Nucleus |
| Dhu000010754 | DhBBX2 | 423 | 46307.13 | 8.36 | 49.48 | 62.41 | −0.39 | Nucleus |
| Dhu000003752 | DhBBX21 | 325 | 34477.85 | 6.01 | 44.93 | 63.2 | −0.258 | Nucleus |
| Dhu000000293 | DhBBX22 | 186 | 20983.68 | 6.4 | 56.19 | 73.33 | −0.507 | Nucleus |
| Dhu000010883 | DhBBX17 | 508 | 55543.31 | 7.11 | 48.29 | 68.62 | −0.412 | Nucleus |
| Dhu000023905 | DhBBX9 | 208 | 22656.72 | 6.97 | 48.15 | 74.62 | −0.256 | Nucleus |
| Dhu000021193 | DhBBX8 | 208 | 22612.66 | 6.97 | 48.15 | 74.18 | −0.255 | Nucleus |
| Dhu000003422 | DhBBX18 | 499 | 54675.09 | 7.46 | 53.79 | 67.13 | −0.519 | Nucleus |
| Dhu000014192 | DhBBX5 | 146 | 15992.6 | 8.42 | 47.37 | 96.37 | 0.19 | Nucleus |
| Dhu000023330 | DhBBX10 | 488 | 53490.13 | 5.99 | 44.43 | 68.83 | −0.284 | Nucleus |
| Dhu000002829 | DhBBX4 | 226 | 24826.28 | 4.95 | 73.99 | 57.57 | −0.746 | Nucleus |
| Dhu000010227 | DhBBX19 | 203 | 22095.56 | 5.15 | 61.71 | 65.96 | −0.427 | Nucleus |
| Dhu000001125 | DhBBX6 | 366 | 40868.9 | 7.07 | 60.8 | 63.99 | −0.733 | Nucleus |
| Dhu000013676 | DhBBX7 | 366 | 40998.11 | 7.56 | 62.85 | 65.85 | −0.716 | Nucleus |
| Dhu000000981 | DhBBX1 | 238 | 25553.79 | 4.6 | 65.52 | 51.81 | −0.653 | Nucleus |
| Dhu000000066 | DhBBX20 | 237 | 25989.73 | 4.78 | 57.45 | 66.75 | −0.392 | Nucleus |
| Dhu000010353 | DhBBX11 | 281 | 31594.37 | 5.25 | 62.09 | 64.23 | −0.583 | Nucleus |
| Dhu000023175 | DhBBX12 | 281 | 31594.37 | 5.25 | 62.09 | 64.23 | −0.583 | Nucleus |
| Dhu000022626 | DhBBX15 | 395 | 42293.61 | 6.31 | 53.45 | 64.63 | −0.45 | Nucleus |
| Dhu000018351 | DhBBX16 | 395 | 42252.43 | 5.9 | 55.09 | 64.63 | −0.462 | Nucleus |
| Dhu000024355 | DhBBX14 | 166 | 18528.03 | 4.94 | 49.19 | 84.04 | −0.256 | Nucleus |
| Dhu000020406 | DhBBX13 | 187 | 21036.62 | 4.86 | 58.22 | 75.61 | −0.408 | Nucleus |
| Dhu000003374 | DhBBX23 | 140 | 16008.51 | 6.43 | 69.89 | 87.79 | −0.013 | Nucleus |

categorized into four distinct classes based on their domain arrangements: those possessing a single B-box domain, those with dual B-box domains, those combining a B-box with a CCT domain, and those equipped with two B-box domains accompanied by a CCT domain. Homologs from both *D. huoshanense* and *A. thaliana* genomes were carefully selected to explore the evolutionary and functional relationships among *BBX* genes. Their multiple sequence alignment and subsequent phylogenetic tree analysis aimed to unravel insights into the evolutionary dynamics and potential functional distinctions within this gene family. (Fig. 1). Considering the disparities in protein topological architecture, this research delineated the BBX family grouped into five distinct and highly conserved subfamilies, each corroborated by strong bootstrap validation. Based on our investigation, the phylogenetic tree classified the BBX into five groups based on clades. Notably, Groups I, IV, and V were distinguished by a significant number of *DhBBX* members, while subfamily III comprised a more limited representation with only five members. Subfamilies III had included both domains the BBX and CCT. In addition, the only CCT domain-related genes found in subfamily II and subfamily III. A significant portion of BBX genes possessing two B-box domains fell within a specific subfamily I. Almost all subfamilies belong to BBX, except II and III. In addition, we examined the *D. huoshanense* BBX genes to investigate their evolutionary connection to *A. thaliana* BBX members. In this research, we discovered that the *A. thaliana* BBX genes and *D. huoshanense* BBX genes were clustered together and showed a strong relationship.

### 3.3. Microsynteny, gene duplication events and chromosomal localization of DhBBXs

The chromosomal distribution and gene duplication occurrences of *DhBBX* genes were examined to shed more light on how these genes evolved. There are 17 chromosomes total, and nine of them were discovered to include 23 *DhBBX* genes (Fig. 2). Four *DhBBX* genes among them were found on chromosome 16, followed by chromosomes 3, 6, and 8, which each had three *BBX* genes. Only two genes were embedded on chromosomes 7, 10, 11, and 18, and just one gene on chromosome 1.

Several *DhBBX* genes, including *DhBBX17, DhBBX18, DhBBX19, DhBBX20,* and *DhBBX21* were grouped together on chromosome 16, likely due to tandem duplication events. Tandem and segmental duplication are typically used to expand gene families. We were unable to locate any tandem duplication pairings in the current investigation. The gene pair collinearity in the genome of *D. huoshanense* was analyzed through the MCScanX software. *Dhu000003752, Dhu000000066, Dhu0000010227, Dhu000003422* and *Dhu0000010883* showed microsynteny with *Dhu000000981, Dhu000010754, Dhu000000904* and *Dhu000002829* genes situated on

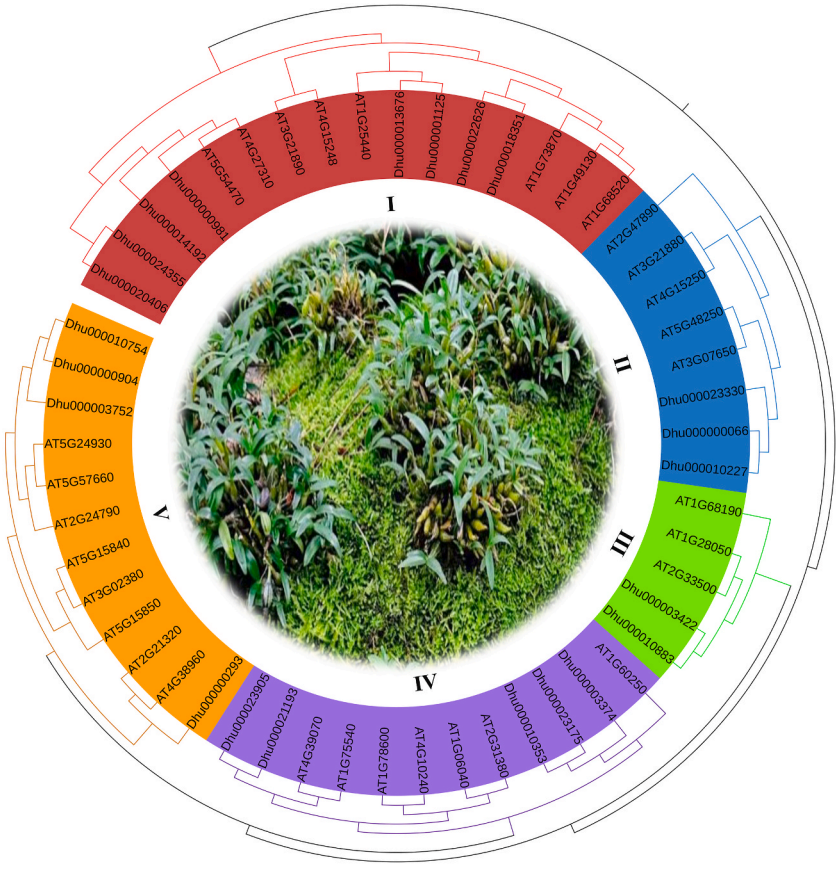


**Fig. 1.** Phylogenetic tree of *DhBBXs* genes from *D. huoshanense* and *A. thaliana*. The construction of the phylogenetic tree was facilitated by the MEGA 7.0 software, utilizing full-length protein sequences for the analysis. The Maximum Likelihood method was applied, and the reliability of the tree was assessed using 1,000 bootstrap replicates.

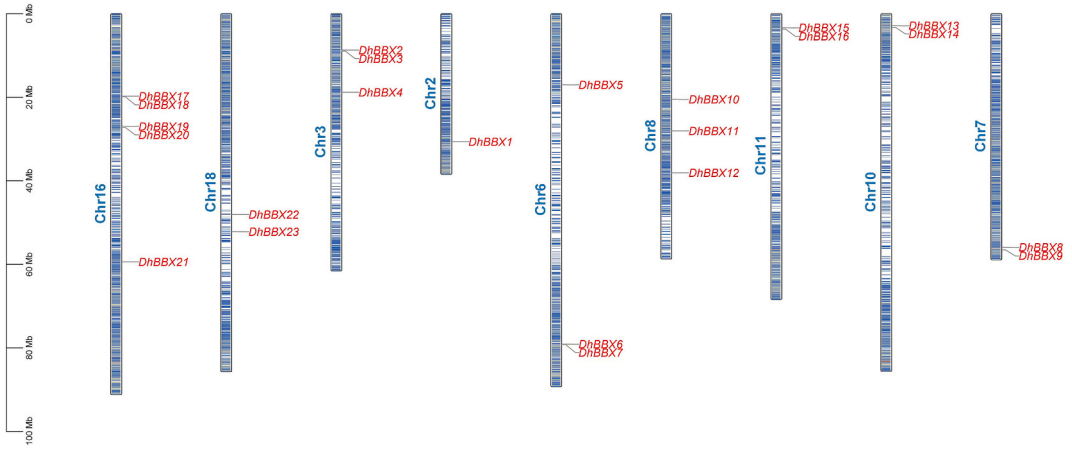


**Fig. 2.** The chromosomal mapping and distribution of *BBX* genes in the *D. huoshanense* genome. Each chromosome is represented by a vertical blue bar, the numerical designation of which is conspicuously displayed on the left-hand side of the bar. These numerical designations serve as a means of identification, aiding in the explication and differentiation of the individual chromosomes.

chromosomes 2, 3, and 18. Notably, genes *Dhu000000981, Dhu000010754, Dhu000000904* and *Dhu000002829* also showed microsynteny with *Dhu000020406* and *Dhu000024355*. Microsynteny studies revealed pronounced collinearity for *DhBBX* genes situated on chromosomes 2, 3, 6, 7, 8, 11, and 18 (Fig. 3). Additionally, a collinear relationship was identified between *Dhu000023905* and *Dhu000021193*.

We conducted comparative genomics analyses involving *D. huoshanense, D. nobile, O. sativa, D. chrysotoxum,* and *A. thaliana* to elucidate the evolutionary and orthologous gene connections between various species, as well as to explore the emergence and numerous functional divergences of BBX homologous members (Fig. 4 and Table S2). We observed more extensive synteny blocks between *D. huoshanense* and *D. nobile*, and between *D. huoshanense* and *D. chrysotoxum* comprising 20 and 21 pairs, respectively. This pattern was followed by *D. huoshanense O. sativa*, *D. huoshanense* and *A. thaliana*, which exhibited 7 and 6 pairs, respectively. These findings align with the established evolutionary relationships among these species.

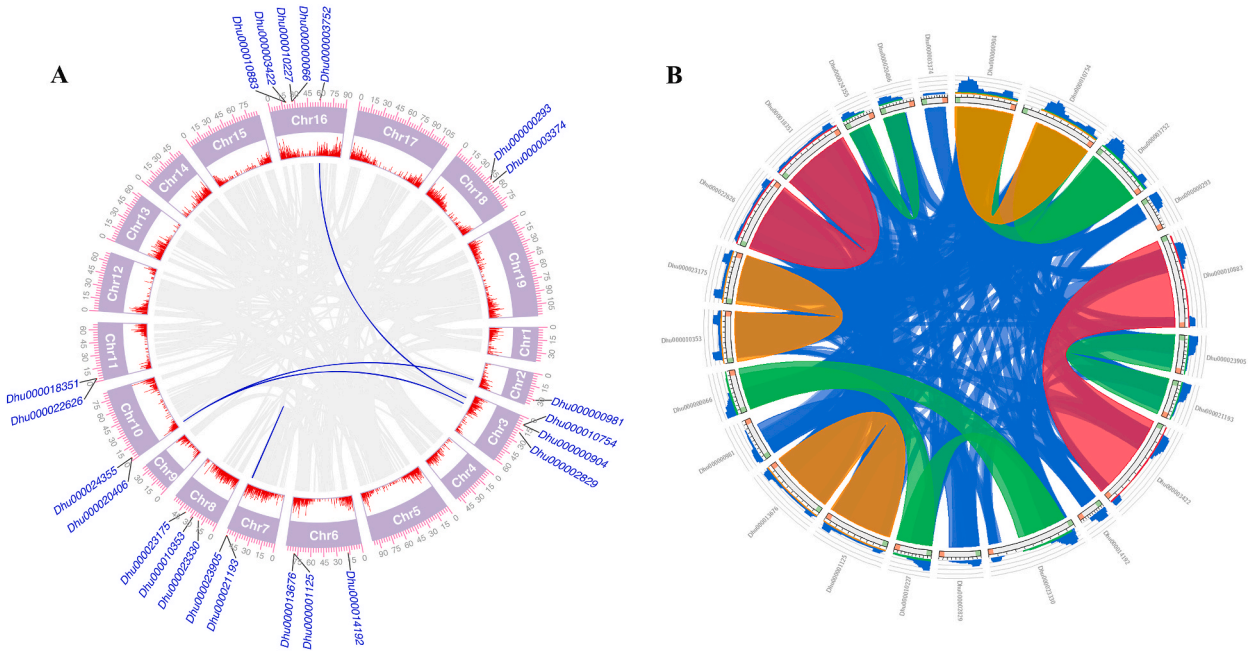


**Fig. 3.** Microsynteny analysis of *BBXs* genes within the *D. huoshanense* genome. (A) Employing a multi-layered visual representation to illuminate the intricacies of gene duplication, chromosomal length, gene density, and syntenic relationships. Duplicated blocks within the chromosomes are delineated by blue lines, offering a visual cue to identify regions of genetic redundancy or repetition. (B) Synteny relationship between *BBX* genes of *D. huoshanense*.

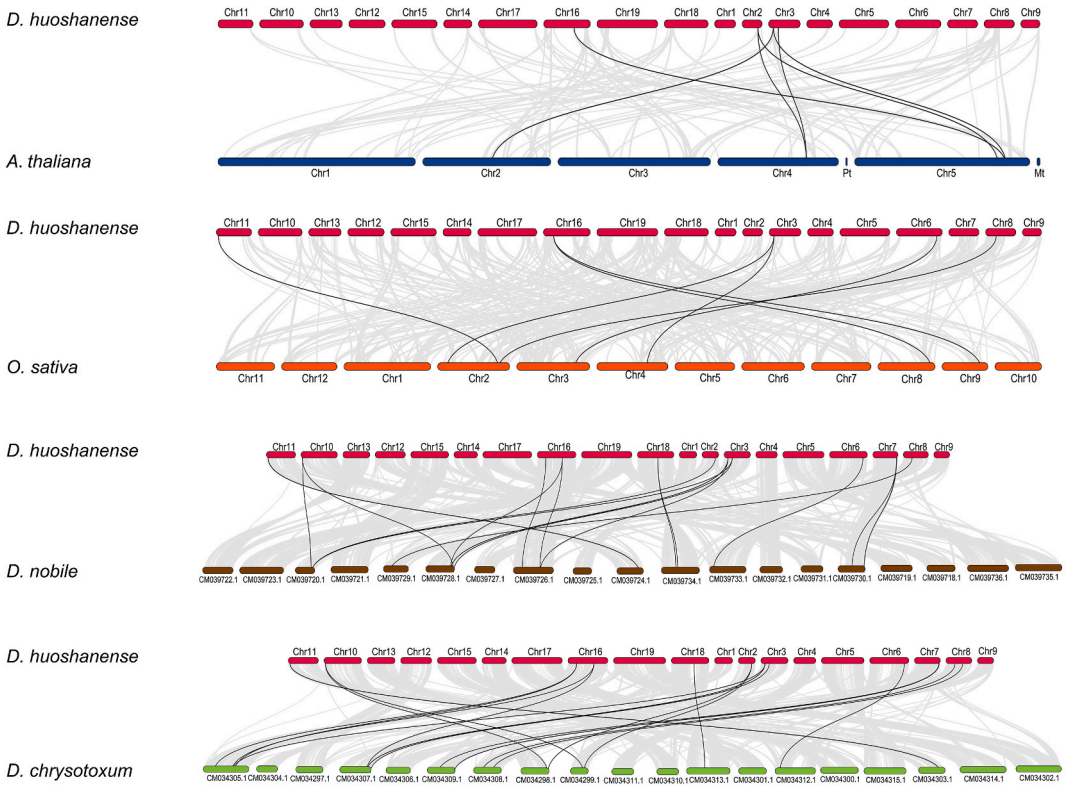


**Fig. 4.** Comparative genomic analysis performed on *D. huoshanense* genes between *D. huoshanense* and *A. thaliana*, *D. huoshanense* and *O. sativa*, *D. huoshanense* and *D. nobile*, *D. huoshanense* and *D. chrysotoxum*. Black lines specifically highlight the collinear gene pairs that include members of the *DhBBXs* gene family.

### *3.4. Gene structure and conserved motif analysis of DhBBXs*

The *DhBBX* genes, based on their chromosomal location and annotation, appear to be sporadically distributed throughout the chromosomes of the examined species. A multi-gene family's evolution may be facilitated by gene structural diversity, according to earlier studies [34]. Gene exon-intron analysis was done in order to characterize and comprehend the structural diversity of the *DhBBX* genes (Fig. 5). Upon detailed scrutiny of the gene structure, it is apparent that the *DhBBXs* feature complete open reading frames, including untranslated regions (UTRs), exons, and introns. A majority of the *DhBBX* genes were characterized by the presence of multiple exons and introns (Fig. 5). The phylogeny analysis revealed that *DhBBX* genes with significant similarity shared comparable exon and intron configurations. Similarly, when examining conserved motifs, it was evident that *DhBBX* genes originating from the same branch displayed similar motif arrangements. The number of exons ranged from 1 to 5, and *Dhu000023330* has the most exons and introns of all the *DhBBX*. On the other hand, *Dhu000014192* has one exon (Fig. 5).

In addition, *DhBBX* genes were found to be grouped in one clade with a strikingly similar exon-intron structure. For instance, *Dhu000010883* and *Dhu000003422* had 4 exons. These findings demonstrated exon loss or gain during the evolution of the *DhBBX* gene family, which led to functional divergence among the closely related *DhBBX* (Fig. 5). Utilizing the MEME Suite tool, we identified twenty representative motifs within *DhBBX*. Motifs 1, 2, and 6 were prevalent in the majority of *DhBBX* genes, representing the standard structures associated with BBX and zinc-finger domains. Additionally, unique motifs were discovered in specific *DhBBX* genes. Notably, the highest motifs were present in *Dhu000010883* and *Dhu000003422*. As well as the lowest motifs were identified in *Dhu000003374* and *Dhu000014192* (Fig. 5). These distinctive patterns were associated with the diverse functionalities of the BBX genes. According to these findings, the *DhBBX* gene family had undergone exon loss or exon gain during its evolution, which caused the functional divergence among the closely related *DhBBXs*.

### *3.5. Cis-elements analysis of DhBBXs genes*

To unravel regulatory elements and functions, we conducted an analysis of the *cis*-acting elements present in the promoter regions of *DhBBX* genes. These promoter regions in *DhBBX* were found to encompass a wide array of regulatory elements associated with processes related to multiple hormones, growth, and development, secondary metabolism, as well as abiotic stress responses (Fig. 6A). We identified a total of 67 distinct *cis*-acting elements, which were classified into different types (Table S3). Notably, a significant number of these elements were associated with processes such as ABA response (ABRE motif), anaerobic induction (ARE motif), and

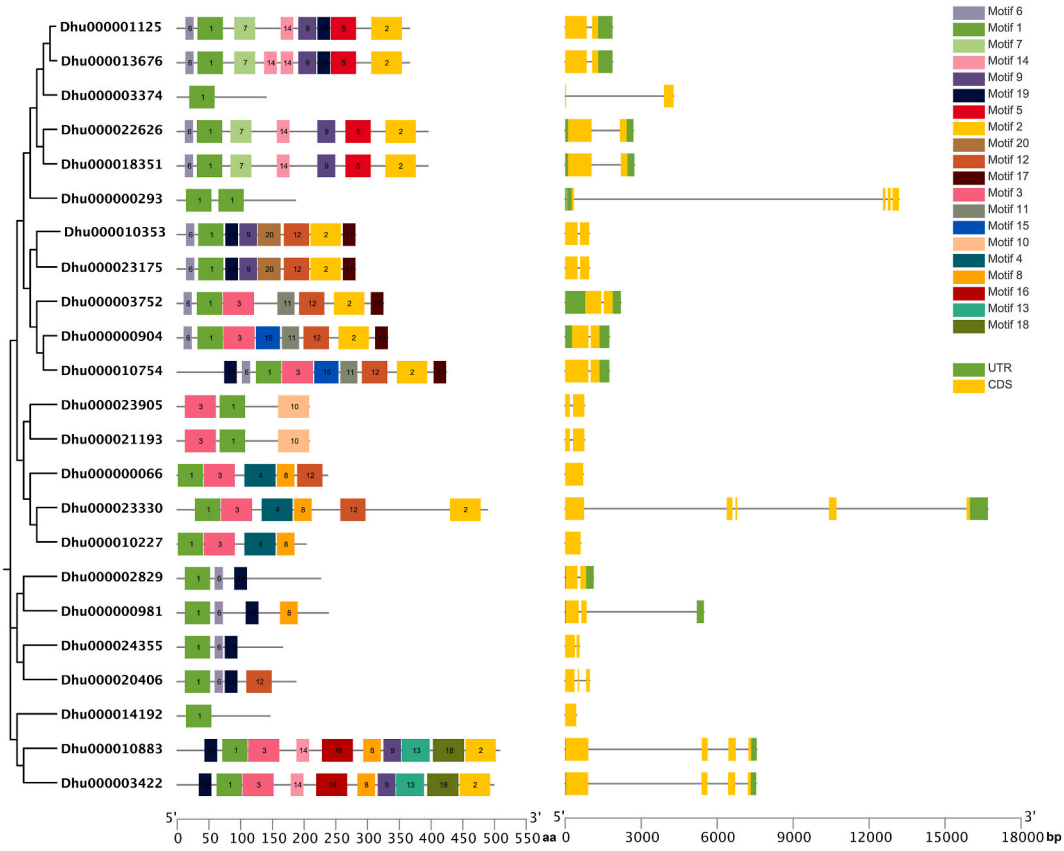


**Fig. 5.** Phylogeny, conserved motifs and gene structural elements within the *DhBBXs*.

light response (including the G-box motif and Box 4 motif), respectively. Hormonal response elements, such as ABRE (48) related ABA response element, CGTCA-motif (32) related to the MejA response element), and GARE-motif (5) related to the gibberellin response (Fig. 6B). Light-responsive elements are G-box element (40). The meristematic expression-related elements are TGACG-motif (32) plays a key role in *DhBBXs* gene regulation of plant meristem and organogenesis. Stress-related elements, such as MBS (11) as well as some other additional regulatory variables like GC motif (2) and circadian (5) have major functions in anoxic, zein metabolism regulation. Nonetheless, the configurations of *cis*-acting elements among the majority of closely related *DhBBX* members exhibited variations, showcasing a range of *cis*-elements. This observation highlights the concept that despite originating from a common ancestor through duplication of genes, paralogous genes maintain unique and closer functions and are subject to varying degrees of regulatory control.

### 3.6. Functional annotation of DhBBX genes

The gene ontology enrichment analysis unveiled associations with cellular components, molecular and biological processes, with an additional sixteen groups identified as pivotal players in plant molecular functions. When examining the biological processes governed by *DhBBXs* participate in the regulation of flower development, regulation of photomorphogenesis, regulation of flower development, red light signaling pathway, regulation of photomorphogenesis, regulation of DNA-templated transcription, photomorphogenesis, and regulation of DNA-templated transcription (Fig. 7). DhBBXs regulate a variety of biological processes, including zinc ion binding, transcription *cis*-regulatory region binding, protein binding, DNA-binding transcription factor activity, and zinc ion binding. In addition to their roles in biological processes, DhBBX proteins were identified as being engaged in the regulation of various molecular functions. Additionally, the GO (gene ontology) enrichment analysis predicted the involvement of *DhBBXs* protein in processes related to the nucleus, chloroplast, and cytoplasmic (~5 %) compartments, as detailed in Table S4. Predictions for subcellular localization showed that the majority of *DhBBX* proteins were found in the nucleus and chloroplast, with only one localized in the Cytoplasm.

### 3.7. Expression profiles of DhBBX genes

To get a full picture of the effects of methyl jasmonate (MeJA) treatment, we did a comparative transcriptomic analysis that covered

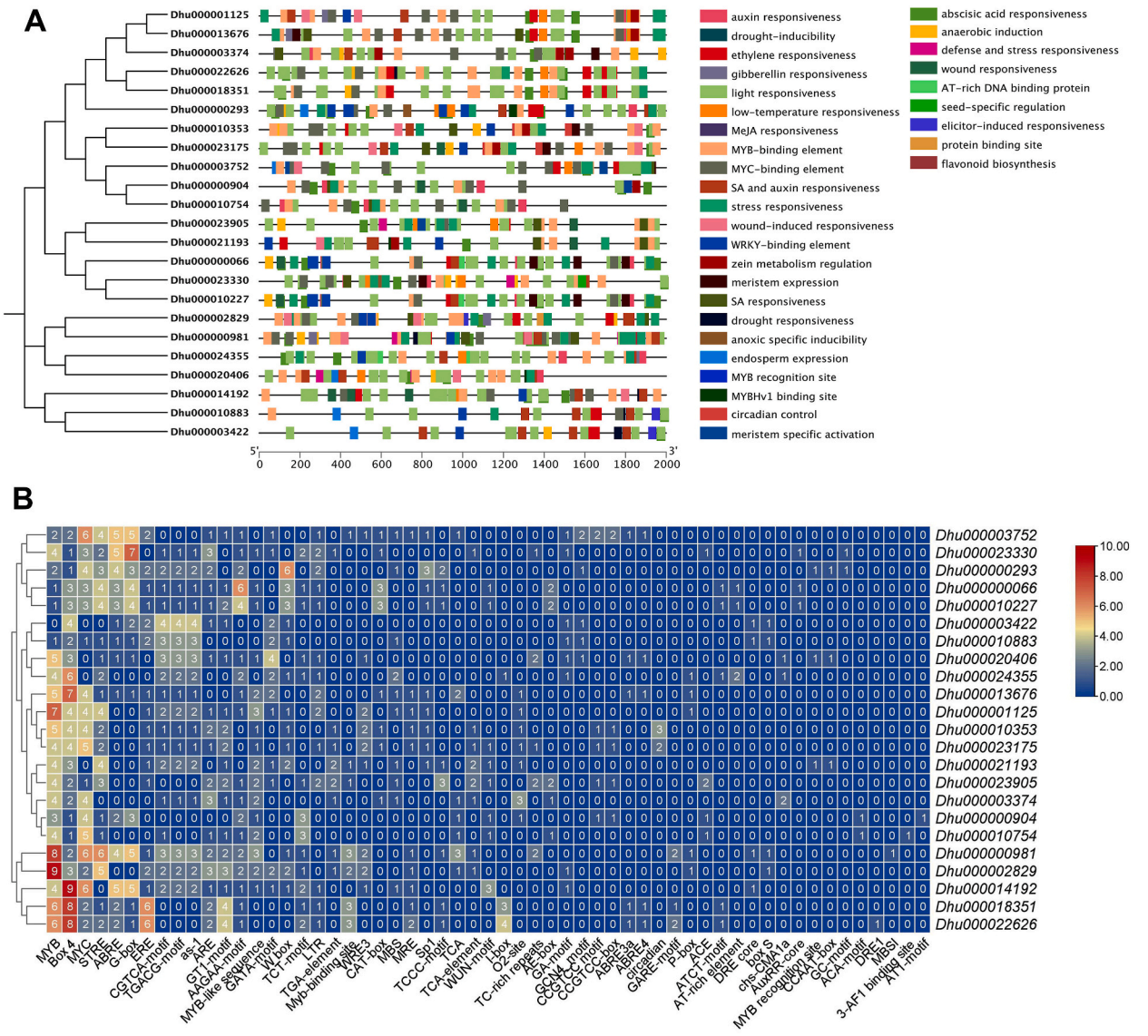


**Fig. 6.** Prediction of *cis*-acting elements in the promoter regions of *DhBBXs* genes. (A) The *cis*-elements are predicted using a 2000bp sequence of promoter region of *DhBBX* genes and are visually represented as colored ellipses. (B) Composition and number of *cis*-acting elements in the promoter of *DhBBX* genes.

16 h of exposure. We carefully looked at the expression profiles of 15 *DhBBXs* genes using sequences from clean reads that had been carefully filtered (Table S5). After subjecting these genes to heatmap clustering analysis, we discovered distinct patterns of the genes with consistently high expression levels at the Time6-vs-Time7 intervals, such as *Dhu000023330, Dhu000018351, Dhu000021193, Dhu000023905,* and *Dhu000003422* (Fig. 8).

Notably, the influence of MeJA treatment was profound, as evidenced by the robust induction of *Dhu000010227, Dhu000020406, Dhu000024355,* and *Dhu000013676,* whereas *Dhu000000904, Dhu000010883, and Dhu000000066, Dhu000010353, Dhu000022626,* and *Dhu000003374* exhibited no discernible response to MeJA treatment. Furthermore, the expression profile of *DhBBX* genes were employed at various time points (Fig. 8). The majority of *DhBBX* genes exhibited upregulated expression at 0.25 h (Time 2) after treatment, with the highest expression observed at 4 h (Time 6). Remarkably, *Dhu000021193* showed the most expression of fold change (highlighted by the red block) when revealed after 8 h of MeJA treatment (Time 7), signifying a significant upregulation in its expression. Conversely, *Dhu000024355* displayed the most pronounced fold change after just 2 h of treatment (Time 3), implying a potent inhibitory effect of MeJA on its expression. Our findings suggest that *DhBBX* genes might reveal its special behavior to JA signaling.

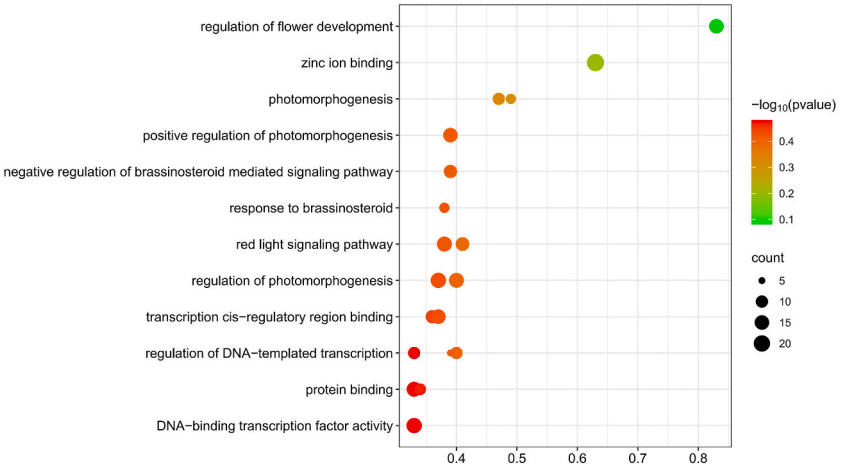


**Fig. 7.** Analysis of the Gene Ontology (GO) annotations for *DhBBXs* proteins. GO annotation was conducted across three distinct categories: biological process, cellular component, and molecular function. The dot in the graphical representation displays the proportion of predicted proteins in terms of percentages for each category.

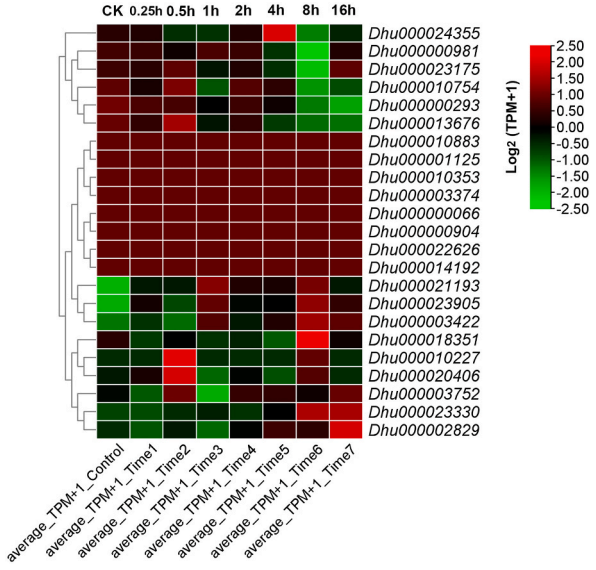


**Fig. 8.** The heatmap of expression profile of *DhBBXs* genes at different time with MeJA treatment. Expression changes are quantified using fold changes, which have been normalized using the logarithm base 2 function of the ratio of FPKM values between two comparative groups.

### *3.8. Expression analysis of DhBBX genes under abiotic stresses*

A comprehensive investigation was undertaken to analyze the expression patterns of *DhBBX* genes through qRT-PCR. This meticulous assessment was conducted following the application of distinct exogenous hormones (ABA, IAA, MeJA, SA, GA) and exposure to cold stress in *D. huoshanense* at different time intervals. This time point was strategically chosen due to its correlation with the peak hormonal activity in *D. huoshanense*. The overarching objective of this investigation was to gain deeper insights into the dynamic expression levels of *DhBBX* genes when exposed to stress-related hormones. It is worth noting that the response dynamics were meticulously monitored at multiple time intervals, including 2 and 8 h, but ABA hormone on 2 and 4 days (Fig. 9). The outcomes of this endeavor unveiled a notable alteration in the expression profiles of *DhBBX* members across the spectrum of multiple hormones and time points. This intricate interplay between genes and hormonal stimuli provides valuable insights into the molecular responses of *D. huoshanense* under the influence of these stress-related hormones. We observed that the *DhBBX* genes exhibited unique and nuanced responses to each hormone intervention. Under ABA treatment, *Dhu000000293* and *Dhu000023330* showed a substantial surge in expression on the 2nd, while *Dhu000000066, Dhu000000904, Dhu000003752,* and *Dhu000010227* exhibited little expression on different levels (Fig. 9A). On the other hand, IAA treatment had no significant expression (Fig. 9B). GA treatment led to the

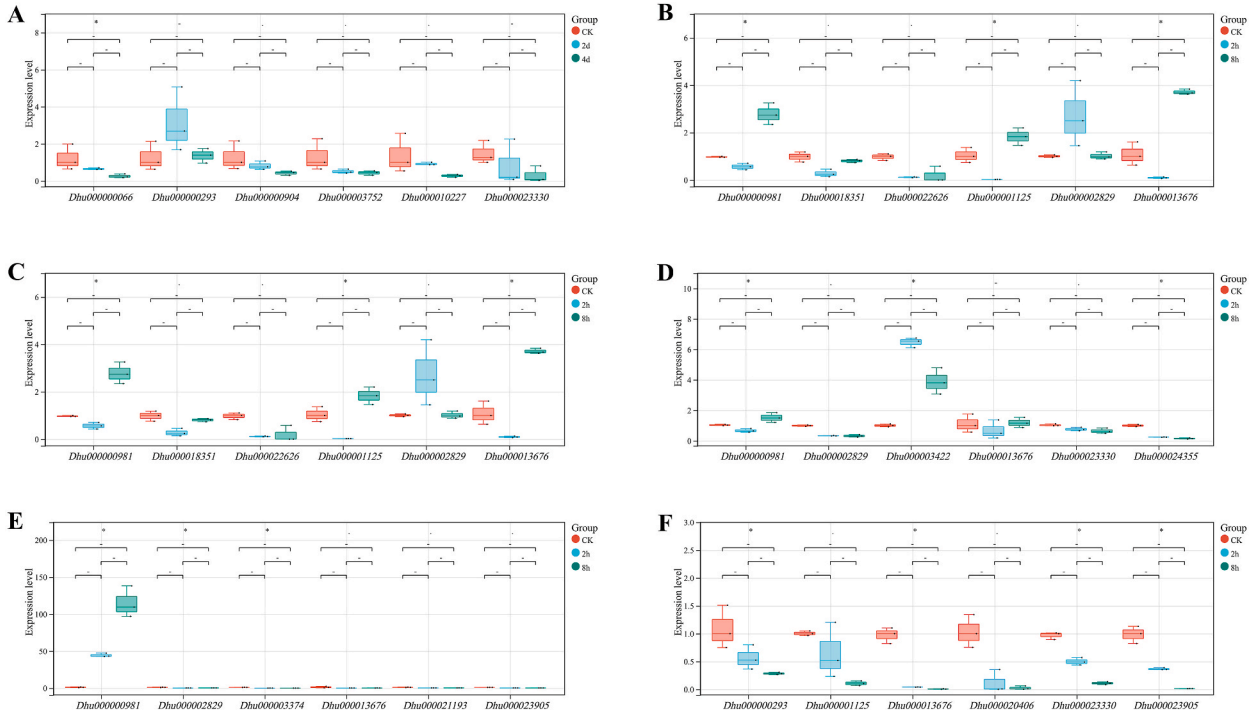


**Fig. 9.** The expression levels of *DhBBXs* genes in *D. huoshanense* under six distinct types of abiotic stressors (ABA, GA, IAA, MeJA, SA, and cold stress). The quantification of gene expression is achieved through quantitative reverse transcription polymerase chain reaction (*q*RT-PCR), and the actin gene serves as the normalization control. (A) The seedlings are exposed to abscisic acid (ABA) treatments, with the time frames of exposure categorized as CK (control), 2 days, and 4 days. (B) Delineates the gene expression patterns under indole-3-acetic acid (IAA) treatments at distinct intervals labeled as CK, 2 H, and 8 H. (C) The effects of gibberellic acid (GA) treatments on *DhBBXs* gene expression, with observations taken at CK, 2 H, and 8 H. (D) Explores the impact of Methyl Jasmonate (MeJA) treatments, with temporal markers set at CK, 2 H, and 8 H. (E), The seedlings undergo salicylic acid (SA) treatments, and gene expression is recorded at CK, 2 H, and 8 H. (F) The *DhBBXs* gene expression changes under cold stress conditions, specifically at 4 °C, with time points at CK, 2 H, and 8 H. Statistical rigor is maintained through the inclusion of error bars, which are calculated based on three biological replicates for each treatment. Significance levels are denoted by asterisks placed atop the error bars, providing a visual cue for statistical validity. A single asterisk (*) indicates a significance level where $P < 0.05$; two asterisks (**) signify $P < 0.01$; and three asterisks (***) represent an even more stringent significance level with $P < 0.001$.

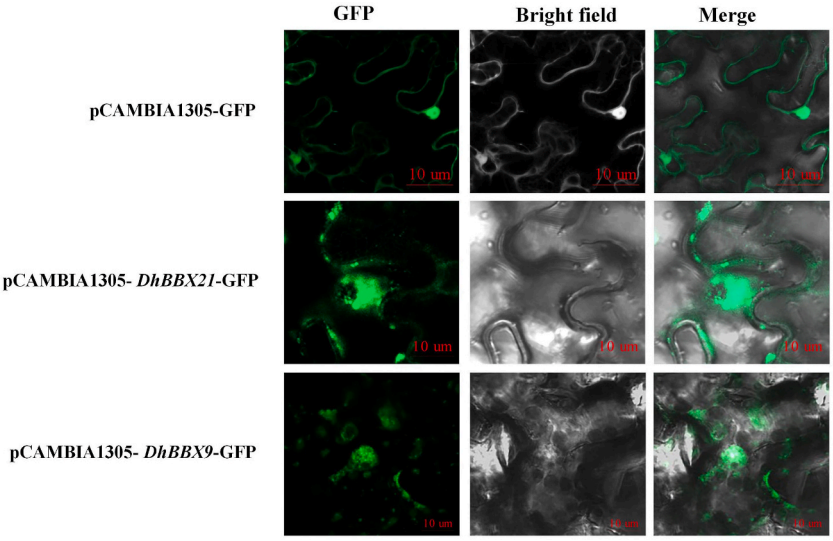


**Fig. 10.** Subcellular localization analysis of DhBBX proteins. Subcellular localization of pCAMBIA1305-DhBBX21-GFP and pCAMBIA1305-DhBBX9-GFP. GFP: green fluorescence signal, Bright Field: bright field, Merge: superposition field. The scale bar is 10 μm.

heightened expression of *Dhu000000981*, and *Dhu000001125* on the 16 h, while *Dhu000013676* showed the highest expression on 16 h as compared to other genes (Fig. 9C). *Dhu000002829* showed the highest gene expression at 2 h. Meanwhile, the application of MeJA resulted in the significant upregulation of *Dhu000000981* on the 2 h, while the *Dhu000003422* gene continued to exhibit heightened expression on the 2 h and 16 h of treatment (Fig. 9D). Under the influence of SA, *Dhu000000981* initially elevated in expression at the 2 h and 16 h but rebounded with the heightened expression in the 8 h (Fig. 9E). The cold stress conditions revealed that all genes had little expression as compared to the control (Fig. 9F). These empirical findings serve to substantiate the broad-ranging involvement of *DhBBX* genes in the intricate process of development, underscoring their pivotal role in responding to abiotic stressors.

### *3.9. Subcellular localization of DhBBX21 and DhBBX9*

To figure out the functional location of the DhBBX proteins in cells, two target genes were connected to the pCAMBIA1305-GFP subcellular localization vector. The results showed that the empty fluorescent signal was distributed in the nucleus, cytoplasm, and cell membrane. The fluorescent signal of pCAMBIA1305-*DhBBX21*-GFP was localized on the nucleus and cytoplasm, which indicated that the DhBBX21 protein mainly functions on the nucleus and cytoplasm. The fluorescent signal of pCAMBIA1305-*DhBBX9*-GFP also localized on the nucleus, which suggested that the DhBBX9 protein mainly functions on the nucleus (Fig. 10).

## 4. Discussion

In recent years, the scientific community has shown a growing fascination with the BBX gene family. Previous research has already delved into the identification of BBX genes throughout the entire genome of rice [42] as well as other significant plants such as potato, Arabidopsis, apple, tomato, and pear [43–47]. The comprehensive genome-wide identification of *BBX* genes in *D. huoshanense* was conducted, with a specific focus on their responses to various hormone treatments (ABA, GA, IAA, MeJA, and SA). Additionally, we analyzed their expression responses under cold stress conditions. Notably, genome duplication events emerged as the prevailing mechanism, potentially playing a pivotal role in the proliferation of *DhBBXs*. Microsynteny analysis involving *D. huoshanense*, *A. thaliana*, *O. sativa*, *D. nobile*, and *D. chrysotoxum* revealed that duplicated regions of DhBBXs remained highly conserved and experienced purifying selection throughout their evolutionary journey. Moreover, an in-depth examination of their physicochemical characteristics, gene structures, and motifs revealed diversification in terms of quantity, functional divergence, and structural attributes.

The number of *BBX* genes exhibits some variation across various crops, with rice, Arabidopsis, tomato, and potato having 30, 32, 29, and 30 members, respectively [48,49]. There is virtually no variation in *BBX* genes between the different plants. But there are 67 *BBX* genes altogether in the apple [50]. Due to the heterozygous nature and large size of the apple genome, there could be differences in the count of *BBX* genes when compared to both tree and crop plants. In our analysis, we identified 23 *BBX* gene members within the *D. huoshanense* genome. Based on domain architecture in tomato and Arabidopsis, previous investigations classified BBX proteins into four distinct categories [51,52].

BBX proteins exhibit a diverse classification into five distinct groups based on their structural features. These include proteins with a single B-box domain, those possessing two B-box domains, proteins with a B-box coupled with additional CCT domains, and those presenting two B-boxes accompanied by supplementary CCT domains. However, we did observe a slight divergence in the composition of one category of BBX proteins across various species. Therefore, it is suggested that during their evolutionary relationship, members of the subfamily BBX had similar gene structures and various functional characteristics. It has also been previously shown that during rice evolution, members of the ferric reduction oxidase family had a similar gene structure and functional features [53]. Furthermore, it has already been noted that the domain of CCT is highly conserved [54]. Still, there is a theory that during evolution, a process called deletion happens, which leads to the creation of a new group of BBX genes that can be identified by their single B-box domain [55]. We have formulated a hypothesis suggesting that a deletion event within the B-box2 domain might lead to the emergence of the B-box1 domain. This hypothesis stems from a comprehensive sequence alignment of the two B-box domains (B-box1 and B-box2), which revealed a higher level of conservation in the B-box1 domain within rice *BBX* genes. Throughout the course of evolution, these gene family members undergo amplification in the genome through both tandem duplication processes and large-scale duplication [56]. On chromosomes, tandem duplications of the genes were also found, which most likely aided in the production and functionalization of paralogous genes. To reveal orthologous genes and explore the evolutionary connections between diverse species, as well as to examine the origins and functional differentiation of BBX homologous genes, we conducted comprehensive comparative genomics analyses that included *D. huoshanense, A. thaliana, O. sativa, D. nobile,* and *D. chrysotoxum* (Fig. 4). At closer distances, orthologous gene pairs were more commonly observed. These findings support the idea that gene duplication expedited species development and provided the basis for the creation and neo-functionalization of genes [57].

The majority of plants are vulnerable to biotic and abiotic stress factors, which affect their output and survivability rate during the course of their lives [48]. In response to stress, plants have evolved tolerance mechanisms that alter the biochemistry and physiology of their cells by altering gene expression [50]. A BBX family of transcriptional regulators has 29 members in tomatoes and 32 in Arabidopsis [36,47]. BBXs play an important role in Arabidopsis regulatory networks that affect growth and development processes such as seedling photomorphogenesis, flowering regulation, and avoidance of shade (Khanna et al., 2009; Gangappa & Botto, 2014; Xu et al., 2018). The role of some BBXs in plants' reactions to diverse abiotic stressors has been in-depth investigated in recent years. For instance, *AtBBX5* and *AtBBX21* were positive regulators that regulated Arabidopsis' ability to tolerate salt and drought [58]. Abscisic acid (ABA), a significant phytohormone, is crucial to how plants react to diverse stimuli. Plants always activate the ABA signal transduction pathway to activate the production of stress defense genes in response to abiotic stressors [59]. The transgenic plants

developed a tolerance for abiotic stress as a result of the overexpression of several transcription factor genes [60].

Under ABA treatment, some genes (*Dhu000000293* and *Dhu000023330*) showed a significant increase in expression after 2 h, while others (*Dhu000000066, Dhu000000904, Dhu000003752, and Dhu000010227*) exhibited minimal expression changes. MeJA treatment led to a notable upregulation of *Dhu000000981* at 2 h, and *Dhu000003422* continued to show heightened expression at 2 h and 8 h. Under SA treatment, *Dhu000000981* initially decreased in expression at 2 h but rebounded with higher expression at 8 h. GA treatment resulted in increased expression of *Dhu000000981* and *Dhu000001125* at 8 h, with *Dhu000013676* showing the highest expression at 8 h compared to other genes, and *Dhu000002829* exhibiting the highest gene expression at 2 h. Nevertheless, when exposed to cold stress conditions, all genes exhibited barely any alterations in expression levels in comparison to the control. This result could likely be attributed to the existence of the LTR motif in the promoters. These findings emphasize the diverse responses of genes to different treatments, highlighting the complex role of these genes in development and their importance in response to abiotic stressors.

## 5. Conclusion

In-depth analysis of *B-box* (*BBX*) genes in *D. huoshanense* illuminated their multifaceted roles in plant physiology. The study focused on analyzing the functional localization and expression patterns of the *DhBBX* gene in *D. huoshanense*. Various methods such as chromosome localization, gene structure analysis, conserved motif identification, phylogenetic analysis, collinearity analysis, expression profiling, fluorescence quantitative analysis, and tobacco transient transformation were used. A total of 23 *DhBBX* members were identified, and they were categorized into five evolutionary subsets based on phylogenetic analysis. The genes were found to be localized in the nucleus. The majority of the genes had multiple exons, with some variations due to transposon insertion. The expression patterns of these genes were analyzed using qRT-PCR, with a focus on their response to hormone treatments and cold stress. DhBBX21 was found to be located in the nucleus and cytoplasm. The insights gained from their gene structures, coupled with their expression dynamics under varied hormonal and stress conditions, enhance our understanding of their pivotal roles in plant growth, morphogenesis, and stress adaptability. This study not only adds to the current knowledge on BBX genes but also outlines a promising path for future studies, which could lead to new biotechnological applications in plant breeding and molecular genetics in Dendrobium plants.

## Funding

This work was supported by National Key R&D Program of China (2023YFC3503804), Startup fund for high-level talents of West Anhui University (WGKQ2022025), the Open Fund of Anhui Engineering Research Center for Eco-agriculture of Traditional Chinese Medicine (WXZR202318), and Demonstration Experiment Training Center of Anhui Provincial Department of Education (2022sysx033).

## Data availability statement

The raw datasets of transcriptome used in this study was obtained from the NGDC GSA database with accession code CRA006607. All genome sequences used in this study can be downloaded and queried in the NCBI database.

## CRediT authorship contribution statement

**Hui Deng:** Writing – original draft, Visualization, Validation, Software, Methodology, Investigation, Formal analysis. **Yingyu Zhang:** Writing – original draft, Visualization, Validation, Software, Methodology, Investigation, Formal analysis. **Muhammad Aamir Manzoor:** Writing – review & editing, Validation, Software, Investigation. **Irfan Ali Sabir:** Writing – review & editing, Validation, Methodology, Investigation, Formal analysis. **Bangxing Han:** Writing – review & editing, Resources, Project administration, Funding acquisition. **Cheng Song:** Writing – review & editing, Writing – original draft, Supervision, Resources, Project administration, Methodology, Funding acquisition, Data curation, Conceptualization.

## Declaration of competing interest

The authors declare that they have no known competing financial interests or personal relationships that could have appeared to influence the work reported in this paper.

## Appendix A. Supplementary data

Supplementary data to this article can be found online at https://doi.org/10.1016/j.heliyon.2024.e32773.

## References


[1] J. Huang, X. Zhao, X. Weng, L. Wang, W. Xie, The rice B-box zinc finger gene family: genomic identification, characterization, expression profiling and diurnal analysis, PLoS One 7 (2012) e48242.
[2] S. Kumar, G. Stecher, M. Li, C. Knyaz, K. Tamura, X. Mega, Molecular evolutionary genetics analysis across computing platforms, Mol. Biol. Evol. 35 (2018) 1547–1549.
[3] E. Gasteiger, et al., ExPASy: the proteomics server for in-depth protein knowledge and analysis, Nucleic Acids Res. 31 (2003) 3784–3788.
[4] R. Khanna, et al., The Arabidopsis B-box zinc finger family, Plant Cell 21 (2009) 3416–3420.
[5] S.N. Gangappa, J.F. Botto, The BBX family of plant transcription factors, Trends Plant Sci. 19 (2014) 460–470.
[6] J. Huang, et al., Increased tolerance of rice to cold, drought and oxidative stresses mediated by the overexpression of a gene that encodes the zinc finger protein ZFP245, Biochem. Biophys. Res. Commun. 389 (2009) 556–561.
[7] J.M. Gendron, et al., Arabidopsis circadian clock protein, TOC1, is a DNA-binding transcription factor, Proc. Natl. Acad. Sci. U.S.A. 109 (2012) 3167–3172.
[8] P. Wang, et al., Optimising the use of gene expression data to predict plant metabolic pathway memberships, New Phytol. 231 (2021) 475–489.
[9] J. Mistry, et al., Pfam: the protein families database in 2021, Nucleic Acids Res. 49 (2021) D412–D419.
[10] S.R. Cutler, P.L. Rodriguez, R.R. Finkelstein, S.R. Abrams, Abscisic acid: emergence of a core signaling network, Annu. Rev. Plant Biol. 61 (2010) 651–679.
[11] W.-L. Dong, et al., Molecular evolution of chloroplast genomes of orchid species: insights into phylogenetic relationship and adaptive evolution, Int. J. Mol. Sci. 19 (2018).
[12] Z. Chu, et al., Genomic organization, phylogenetic and expression analysis of the B-BOX gene family in tomato, Front. Plant Sci. 7 (2016) 1552.
[13] J. Chen, et al., Molecular characterization and expression profiles of MaCOL1, a CONSTANS-like gene in banana fruit, Gene 496 (2012) 110–117.
[14] H.-R. Cui, Z.-R. Zhang, W. Lv, J.-N. Xu, X.-Y. Wang, Genome-wide characterization and analysis of F-box protein-encoding genes in the Malus domestica genome, Mol. Genet. Genom. 290 (2015) 1435–1446.
[15] C.D. Crocco, J.F. Botto, BBX proteins in green plants: insights into their evolution, structure, feature and functional diversification, Gene 531 (2013) 44–52.
[16] M. Zaynab, et al., CRISPR/Cas9 to generate plant immunity against pathogen, Microb. Pathog. 141 (2020) 103996.
[17] S.B. Cannon, A. Mitra, A. Baumgarten, N.D. Young, G. May, The roles of segmental and tandem gene duplication in the evolution of large gene families in Arabidopsis thaliana, BMC Plant Biol. 4 (2004) 10.
[18] M. Zaynab, et al., Proteomic approach to address low seed germination in Cyclobalnopsis gilva, Biotechnol. Lett. 39 (2017) 1441–1451.
[19] H. Shi, et al., Analysis of QTL mapping for germination and seedling response to drought stress in sunflower (Helianthus annuus L.), PeerJ 11 (2023) e15275.
[20] C. Chen, et al., TBtools: an integrative toolkit developed for interactive analyses of big biological data, Mol. Plant 13 (2020) 1194–1202.
[21] Y. Cao, et al., B-BOX genes: genome-wide identification, evolution and their contribution to pollen growth in pear (Pyrus bretschneideri Rehd.), BMC Plant Biol. 17 (2017) 156.
[22] H. Yan, et al., Nuclear localization and interaction with COP1 are required for STO/BBX24 function during photomorphogenesis, Plant Physiol. 156 (2011) 1772–1782.
[23] D. Xu, Y. Jiang, J. Li, M. Holm, X.W. Deng, The B-box domain protein BBX21 promotes photomorphogenesis, Plant Physiol. 176 (2018) 2365–2375.
[24] Y. Yin, et al., Genome-wide identification and analysis of the BBX gene family and its role in carotenoid biosynthesis in wolfberry (Lycium barbarum L.), Int. J. Mol. Sci. 23 (2022).
[25] M. Zaynab, et al., Role of secondary metabolites in plant defense against pathogens, Microb. Pathog. 124 (2018) 198–202.
[26] J. Wang, et al., Genome-wide characterization and anthocyanin-related expression analysis of the B-BOX gene family in Capsicum annuum L, Front. Genet. 13 (2022) 847328.
[27] K. Urano, Y. Kurihara, M. Seki, K. Shinozaki, 'Omics' analyses of regulatory networks in plant abiotic stress responses, Curr. Opin. Plant Biol. 13 (2010) 132–138.
[28] Y. Wang, et al., MCScanX: a toolkit for detection and evolutionary analysis of gene synteny and collinearity, Nucleic Acids Res. 40 (2012) e49.
[29] Y. Wang, et al., Major latex protein-like protein 43 (MLP43) functions as a positive regulator during abscisic acid responses and confers drought tolerance in Arabidopsis thaliana, J. Exp. Bot. 67 (2016) 421–434.
[30] U. Talar, A. Kiełbowicz-Matuk, J. Czarnecka, T. Rorat, Genome-wide survey of B-box proteins in potato (Solanum tuberosum)-Identification, characterization and expression patterns during diurnal cycle, etiolation and de-etiolation, PLoS One 12 (2017) e0177471.
[31] C. Song, G. Li, J. Dai, H. Deng, Genome-wide analysis of PEBP genes in Dendrobium huoshanense: unveiling the antagonistic functions of FT/TFL1 in flowering time, Front. Genet. 12 (2021) 687689.
[32] U. Talar, A. Kiełbowicz-Matuk, Beyond Arabidopsis: BBX regulators in crop plants, Int. J. Mol. Sci. 22 (2021).
[33] Y. Tang, et al., Genome-wide analysis of WRKY gene family and the dynamic responses of key WRKY genes involved in Ostrinia furnacalis attack in Zea mays, Int. J. Mol. Sci. 22 (2021).
[34] C. Song, et al., Natural composition and biosynthetic pathways of alkaloids in medicinal Dendrobium species, Front. Plant Sci. 13 (2022) 850949.
[35] C. Song, et al., Comparative transcriptomics unveil the crucial genes involved in coumarin biosynthesis in Peucedanum praeruptorum Dunn, Front. Plant Sci. 13 (2022) 899819.
[36] C. Song, et al., Label-free quantitative proteomics unravel the impacts of salt stress on Dendrobium huoshanense, Front. Plant Sci. 13 (2022) 874579.
[37] C. Song, et al., In-depth analysis of genomes and functional genomics of orchid using cutting-edge high-throughput sequencing, Front. Plant Sci. 13 (2022) 1018029.
[38] J. Schultz, F. Milpetz, P. Bork, C.P. Ponting, SMART, a simple modular architecture research tool: identification of signaling domains, Proc. Natl. Acad. Sci. U.S. A. 95 (1998) 5857–5864.
[39] J.-P. Sánchez, P. Duque, N.-H. Chua, ABA activates ADPR cyclase and cADPR induces a subset of ABA-responsive genes in Arabidopsis, Plant J. 38 (2004) 381–395.
[40] A.J. Soitamo, M. Piippo, Y. Allahverdiyeva, N. Battchikova, E.-M. Aro, Light has a specific role in modulating Arabidopsis gene expression at low temperature, BMC Plant Biol. 8 (2008) 13.
[41] A. Shalmani, et al., Genome identification of B-BOX gene family members in seven Rosaceae species and their expression analysis in response to flower induction in Malus domestica, Molecules 23 (2018).
[42] X. Qiao, et al., Gene duplication and evolution in recurring polyploidization-diploidization cycles in plants, Genome Biol. 20 (2019) 38.
[43] L. Nian, et al., Characterization of B-box family genes and their expression profiles under abiotic stresses in the Melilotus albus, Front. Plant Sci. 13 (2022) 990929.
[44] C. Song, et al., The multifaceted roles of MYC2 in plants: toward transcriptional reprogramming and stress tolerance by jasmonate signaling, Front. Plant Sci. 13 (2022) 868874.
[45] L.-J. Qu, Y.-X. Zhu, Transcription factor families in Arabidopsis: major progress and outstanding issues for future research, Curr. Opin. Plant Biol. 9 (2006) 544–549.
[46] J.-H. Min, J.-S. Chung, K.-H. Lee, C.S. Kim, The CONSTANS-like 4 transcription factor, AtCOL4, positively regulates abiotic stress tolerance through an abscisic acid-dependent manner in Arabidopsis, J. Integr. Plant Biol. 57 (2015) 313–324.
[47] M.A. Massiah, et al., Solution structure of the MID1 B-box2 CHC(D/C)C(2)H(2) zinc-binding domain: insights into an evolutionarily conserved RING fold, J. Mol. Biol. 369 (2007) 1–10.
[48] C. Song, et al., The potential roles of acid invertase family in Dendrobium huoshanense: identification, evolution, and expression analyses under abiotic stress, Int. J. Biol. Macromol. 253 (2023) 127599.
[49] I. Muhammad, et al., Comparative in silico analysis of ferric reduction oxidase (FRO) genes expression patterns in response to abiotic stresses, metal and hormone applications, Molecules 23 (2018).

[50] S. Magadum, U. Banerjee, P. Murugan, D. Gangapur, R. Ravikesavan, Gene duplication as a major force in evolution, J. Genet. 92 (2013) 155–161.
[51] Y. Li, et al., Genome-wide analysis of the RING finger gene family in apple, Mol. Genet. Genom. 286 (2011) 81–94.
[52] X. He, et al., The spatiotemporal profile of Dendrobium huoshanense and functional identification of bHLH genes under exogenous MeJA using comparative transcriptomics and genomics, Front. Plant Sci. 14 (2023) 1169386.
[53] M.A. Manzoor, et al., Comprehensive comparative analysis of the GATA transcription factors in four Rosaceae species and phytohormonal response in Chinese pear (Pyrus bretschneideri) fruit, Int. J. Mol. Sci. 22 (2021).
[54] S.C. Lee, S. Luan, ABA signal transduction at the crossroad of biotic and abiotic stress responses, Plant Cell Environ. 35 (2012) 53–60.
[55] M.A. Larkin, et al., Clustal W and clustal X version 2.0, Bioinformatics 23 (2007) 2947–2948.
[56] I. Letunic, P. Bork, Interactive Tree of Life (iTOL) v4: recent updates and new developments, Nucleic Acids Res. 47 (2019) W256–W259.
[57] M. Lescot, et al., PlantCARE, a database of plant cis-acting regulatory elements and a portal to tools for in silico analysis of promoter sequences, Nucleic Acids Res. 30 (2002) 325–327.
[58] F. Jia, B. Wu, H. Li, J. Huang, C. Zheng, Genome-wide identification and characterisation of F-box family in maize, Mol. Genet. Genom. 288 (2013) 559–577.
[59] G. Li, M.A. Manzoor, G. Wang, C. Chen, C. Song, Comparative analysis of KNOX genes and their expression patterns under various treatments in Dendrobium huoshanense, Front. Plant Sci. 14 (2023).
[60] N. Panchy, M. Lehti-Shiu, S.H. Shiu, Evolution of gene duplication in plants, Plant Physiol. 171 (2016) 2294–2316.